Jurnal Polimesin
Department of Mechanical Engineering
State Polytechnic of Lhokseumawe
http://e-jurnal.pnl.ac.id/polimesin

e-ISSN : 2549-1999 No. : 3 Month : June
p-ISSN : 1693-5462 Volume : 24 Year : 2026

Processing dates: received on 2026-1-18, reviewed on 2026-03-24, accepted on 2026-04-12 and online availability on 2026-06-30

Effect of alkali fusion temperature on the synthesis and characteristics of nanosilica from silica sand

Muhammad Sadat Hamzah*, Muchsin, Abdul Muis, Dino Hasyim, Iqrham Dwi Putra Annas, Muhammad Syaiful Fadly, Bakri, Sri Chandrabakty
Department of Mechanical Engineering, Tadulako University, Palu 94148, Indonesia
*Corresponding author: muhsadathamzah@gmail.com

Abstract

The increasing demand for nanosilica in industrial applications has encouraged the utilization of abundant natural silica sand as a sustainable raw material. This study investigates the effect of alkali fusion temperature on the synthesis and characteristics of nanosilica derived from silica sand from Central Sulawesi, Indonesia. A cost-effective, energy-efficient synthesis method is needed to transform raw sand into high-value nanoparticles with controlled morphology. The study employed the alkali fusion method, where silica sand was reacted with NaOH at temperatures ranging from 400°C to 700°C, followed by leaching and titration to pH 7-8 to produce nanosilica. Characterization results via XRF and XRD confirmed that the synthesized nanosilica maintains a high SiO_2 concentration (up to 72.46%) and exhibits a coexistence of amorphous phases and crystalline quartz. Morphological analysis by TEM revealed that increasing the fusion temperature decreases particle size from 18.91 nm at 400°C to 14.00 nm at 700°C, indicating that higher thermal energy promotes structural decomposition. These findings suggest that the alkali fusion temperature is an important parameter for controlling nanosilica dimensions. Further evaluation, including yield and recovery analysis, is required to assess process efficiency and its potential for large-scale applications.

Keywords:
Alkali fusion, silica sand, nanosilica, fusion temperature, nanomaterials.

1 Introduction

Indonesia possesses vast potential in natural mineral resources, particularly oxide materials such as silica sand [1, 2]. These deposits are widely distributed across the archipelago, including significant reserves in Central Sulawesi. Silica sand sourced from this region is characterized by a high silicon dioxide (SiO_2) content, making it an excellent precursor for high-value industrial raw materials, most notably silica nanoparticles (SNP) or nanosilica (NS).

Nanosilica typically exists in three primary crystalline forms: quartz, tridymite, and cristobalite. Due to its superior properties, such as a large specific surface area, high thermal resistance, excellent mechanical strength, and biocompatibility, it has become indispensable in modern industry [3-5]. Its applications span across diverse sectors, including rubber, automotive, electronics, energy storage, paints, and medical fields [6]. Furthermore, SNP is used as a catalyst precursor, adsorbent, and composite filler and has been shown to improve the efficiency of vapor-compression refrigeration cycles [7-9].

Nanosilica can be synthesized using two primary approaches: top-down and bottom-up [10-12]. The bottom-up process involves chemical synthesis using precursors to build particles at the nanometer scale, which provides enhanced electrical, optical, and magnetic properties compared to micrometer-sized materials [13,14]. To date, several methods have been developed for SNP synthesis, including hydrothermal [15], sol-gel [16], sodium silicate solution [17], alkali fusion [18], and precipitation [19]. Traditionally, these processes involve constant stirring to inhibit excessive grain growth. However, many conventional methods still face technical limitations, remarkably low production yields, and limited control over particle size and morphology.

To address these challenges, researchers have explored alternative external influences to refine particle size. For instance, ultrasonic and microwave methods have been applied to hydroxyapatite synthesis [20,21]. At the same time, mechanical and membrane vibrations have been used to control the size of magnetite and metal particles during metallurgical and welding processes [7,22]. Among chemical routes, the alkali fusion method is gaining popularity due to its shorter synthesis time and lower energy requirements [23]. It involves heating the sample to specific temperatures, then precipitating and stirring until the pH is neutral. Despite its efficiency, the impact of fusion temperature, a critical parameter that determines the final phase and particle size, remains under-optimized to maximize its effectiveness.

This study aims to synthesize nanosilica from Central Sulawesi silica sand using the alkali fusion method, specifically investigating the effect of fusion temperature on the resulting particle characteristics. By optimizing the fusion temperature, this research seeks to produce nanosilica with a more controlled morphology and reduced particle size. The results are expected to provide a more efficient, scalable pathway to high-purity nanosilica suitable for advanced industrial applications.

2 Material and methods

2.1 Material preparation

The raw silica sand used in this study was sourced from Donggala Regency, Central Sulawesi, Indonesia. The sand was initially cleaned and dried to remove impurities. To reduce particle size, the dried sand was mechanically milled in a ball mill. The resulting powder was sieved using a sieve shaker, and the fraction passing through a 74 µm sieve (< 200 mesh) was collected as the starting concentrate.

2.2 Synthesis and characterization of nanosilica via alkali fusion

The synthesis of nanosilica was performed using the alkali fusion method, as illustrated in Fig. 1. Initially, the silica sand concentrate was blended with pro-analysis grade sodium hydroxide (NaOH) at a 1:1 weight ratio. This mixture was heated in a furnace to 400°C, 500°C, 600°C, and 700°C for 1 hour to facilitate the activation reaction. Upon cooling, the fused mixture was dissolved in air conditioner (AC) wastewater and placed on a hot plate magnetic stirrer. The solution was maintained at 70°C with a constant stirring speed of 400 rpm for 16 hours. During this stirring period, the solution was titrated with 2 M hydrochloric acid (HCl, 37% pro-analysis) until a neutral pH of 7-8 was achieved, triggering the precipitation of silica gel. The resulting precipitates were subsequently filtered and washed repeatedly with AC water until a pure white color was obtained. Finally, the samples were dried in an oven at 100°C for 15 hours to produce the nanosilica powder.

The physicochemical properties of the synthesized nanosilica were evaluated using several analytical techniques. The elemental and chemical compositions of the samples were determined using X-ray Fluorescence (XRF), which enables both qualitative and quantitative analysis. This technique applies to various sample forms, including powders, liquids, and solids, and is based on the emission of characteristic X-rays upon irradiation with high-energy X-rays, allowing elemental identification and quantification from measured wavelengths and intensities. Meanwhile, the crystal phase

and its purity were identified by X-ray Diffraction (XRD, Bruker D2 Phaser). Characterization was carried out using Cu−Kα radiation (λ = 0.154 nm) in the range 2θ = 5−90°. The speed used was 3°/min, operating at 40 kV and 30 mA. The morphological and microstructural characteristics were examined using Scanning Electron Microscopy (SEM) and Transmission Electron Microscopy (TEM). SEM observations were performed using a JEOL JSM-6510 LA operated at 15 kV and magnifications up to 100× to evaluate the surface morphology of the samples. TEM analysis was performed using JEOL JEM-1400 and FEI Tecnai G2 S-Twin instruments operated at 200 kV to confirm particle shape and to analyze the diffraction patterns. For TEM analysis, the samples were prepared by drop-casting onto carbon-coated copper grids. Furthermore, particle size analysis was conducted using ImageJ and Origin software, enabling quantitative determination of the average grain size and particle size distribution.

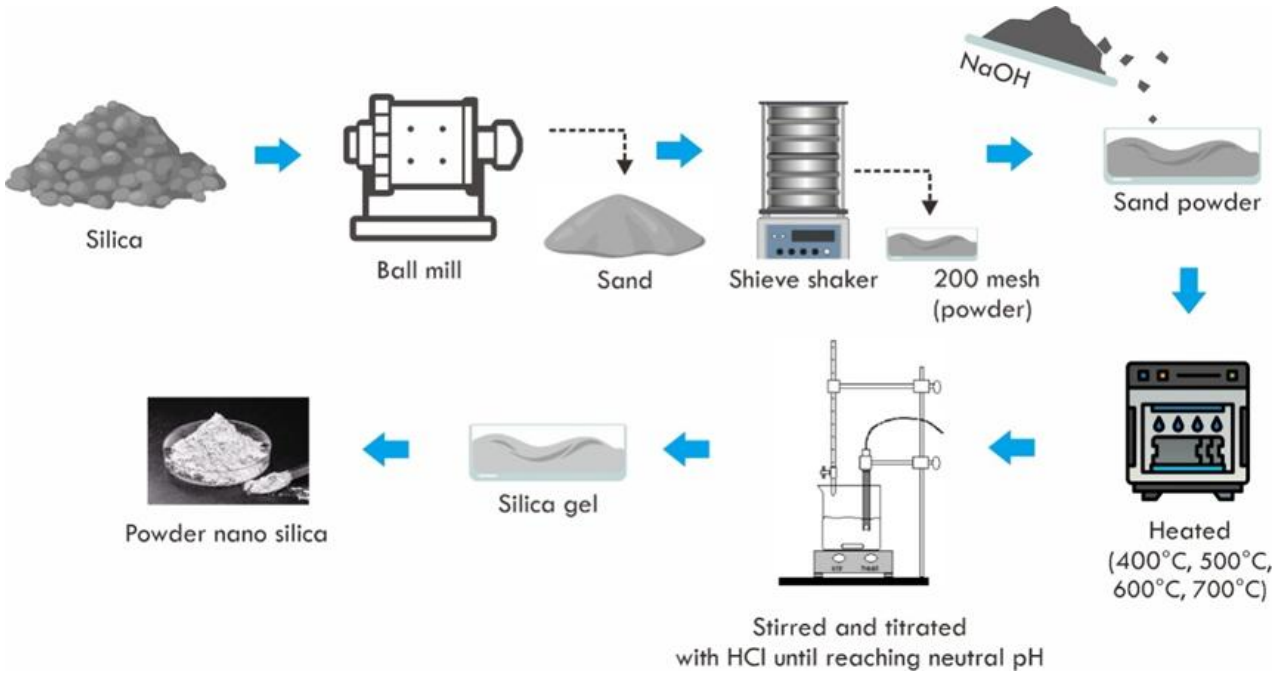

Fig. 1. Schematic diagram of the alkali fusion synthesis process for nanosilica

3 Result and discussion

3.1 Synthesis of nanosilica particles

Nanosilica (NS) was successfully synthesized using the alkali fusion method. During the fusion stage at 600°C, sodium hydroxide (NaOH) reacts with the crystalline silica in the sand to form sodium metasilicate (Na_2SiO_3). This transformation is critical because it converts insoluble silica into a water-soluble form, enabling its separation from mineral impurities. Subsequently, the Na_2SiO_3 solution was titrated with pro-analysis HCl to induce the precipitation of hydrated silica and silicic acid. The resulting white gel-like precipitate was thoroughly washed with AC wastewater to eliminate residual chlorides and soluble impurities. The following equations represent the chemical mechanism of this synthesis:

$$SiO_2 + 2\ NaOH \rightarrow Na_2SiO_3 + H_2O \quad (1)$$

$$Na_2SiO_3 + 2HCl \rightarrow SiO_2 + 2\ NaCl + H_2O \quad (2)$$

3.2 Elemental composition analysis

The chemical compositions of the raw silica sand and the synthesized nanosilica, as determined by X-ray Fluorescence (XRF), are summarized in Table 1. The silica content of the raw material was 70.344%, while the synthesized nanosilica ranged from 69.582% to 72.456%. The results indicate that the primary chemical components remain consistent before and after the synthesis process. This confirms that the alkali fusion method effectively recovers silica from the sand without altering its elemental composition. The results of this study align with previous research, showing that the process of synthesizing nanosilica using the alkali fusion method with membrane vibration did not significantly alter the chemical composition of silica sand [7]. This indicates that the treatment primarily modifies the material's physical structure or particle size, without affecting its primary elemental content.

Table 1. Chemical composition of raw silica sand and nanosilica synthesized at various temperatures.

Composition	Raw material (wt%)	Nanosilica particles (wt%) with alkali temperature 400°C	Nanosilica particles (wt%) with alkali temperature 700°C
SiO_2	70.344	72.456	69.582
Al_2O_3	16.459	18.831	19.6
K_2O	4.254	1.792	1.637
Fe_2O_3	3.970	3.698	4.299
CaO	3.339	2.015	3.283
TiO_2	0.720	0.525	0.852
P_2O_5	0.676	0.421	0.444

3.3 Phase identification and crystallinity

The X-ray diffraction (XRD) patterns of the synthesized nanosilica at various temperatures are shown in Fig. 2. Comparison with JCPDS (card no. 46-1045) and AMCSD databases reveals a coexistence of amorphous and crystalline phases. All samples exhibit a characteristic broad hump centered at $2\theta = 22°$, which is a hallmark of amorphous silica [24,25]. This diffuse scattering pattern is particularly dominant in samples (a) and (b), indicating a high degree of structural disorder.

In addition to the amorphous halo, several sharp diffraction peaks were observed at approximately 2θ = 22-25°, 28-30°, and 50-55°, signifying the presence of a crystalline quartz phase (SiO_2). A prominent peak at $2\theta = 26.70°$, corresponding to the (101) lattice plane, confirms the retention of the quartz structure, which typically forms at temperatures below 870°C [26]. Interestingly, peaks at 21.5°, 31.7°, 42.4°, and 60.2° were found to match the pattern of NaCl [27], likely representing minor residual traces from the titration process. The XRD analysis further suggests that while temperature variations do not fundamentally alter the crystal structure, higher temperatures enhance nucleation rates, potentially leading to a

reduction in crystallite size, as calculated by the Scherrer equation [28].

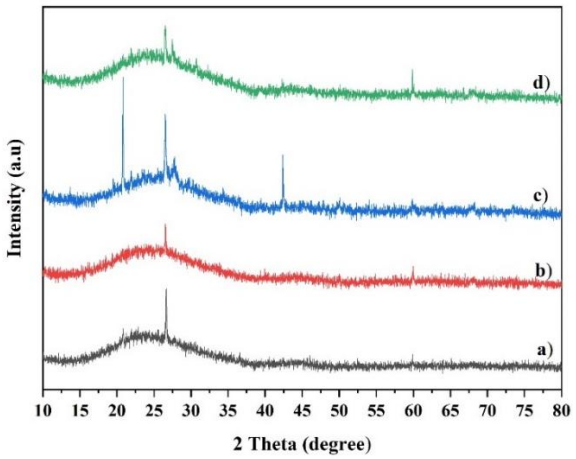

Fig. 2. XRD patterns of nanosilica particles synthesized at different alkali fusion temperatures: (a) 400°C, (b) 500°C, (c) 600°C, and (d) 700°C

3.4 Morphological and microstructural analysis

The surface morphology of the nanosilica was examined using Scanning Electron Microscopy (SEM), as shown in Fig. 3. Samples treated at 400°C and 700°C both exhibit irregular, quasi-spherical shapes with a clear tendency toward agglomeration, a common phenomenon in nanoparticles due to their high surface energy.

To further investigate the internal structure and precise particle size, Transmission Electron Microscopy (TEM) was employed (Fig. 4). The TEM micrographs reveal that the particle size is highly dependent on the alkali fusion temperature. Specifically, the average particle size decreased from 18.91 ± 7.14 nm at 400°C to 14.00 ± 3.33 nm at 700°C. This phenomenon can be attributed to the increased thermal energy at higher temperatures, which promotes a more efficient decomposition of the silica precursor and accelerates the reaction rate between the silica and the alkali. Consequently, higher fusion temperatures facilitate the formation of smaller, more uniform particles, whereas lower temperatures may lead to incomplete reactions and larger, non-homogeneous grain growth.

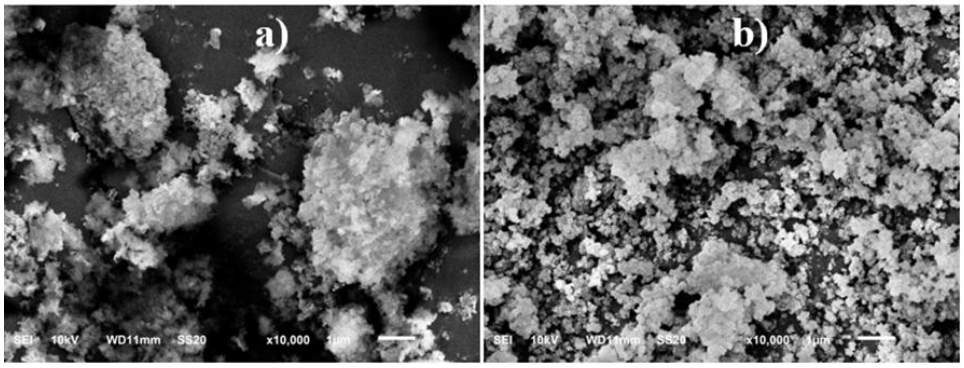

Fig. 3. SEM micrographs of nanosilica particles synthesized at fusion temperatures: (a) 400°C and (b) 700°C (10,000x magnification)

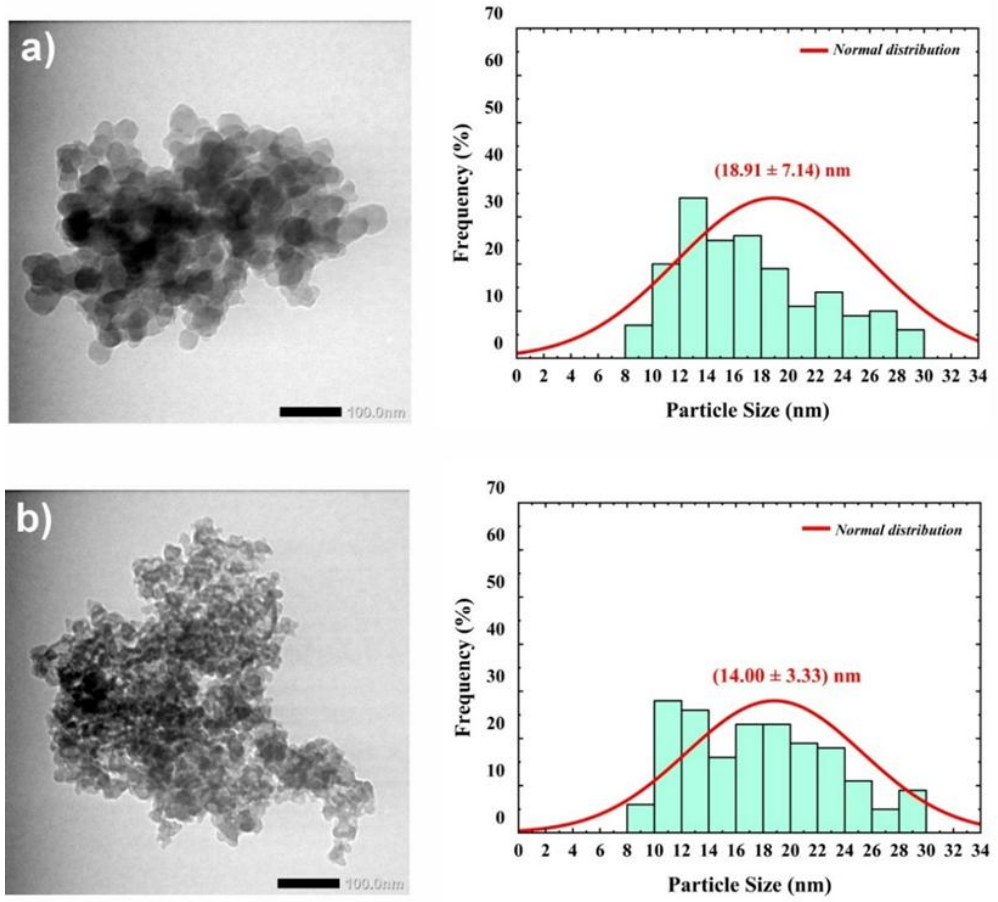

Fig. 4. TEM micrographs and corresponding particle size distributions of nanosilica synthesized at fusion temperatures: (a) 400°C and (b) 700°C

4 Conclusion

This study synthesized nanosilica from Donggala silica sand using an alkali fusion process. XRF analysis indicated a relatively high SiO_2 content of up to 72.46%, while XRD results revealed the coexistence of amorphous and crystalline quartz phases, indicating partial structural transformation during synthesis. TEM observations showed that increasing the fusion temperature from 400°C to 700°C reduced the average particle size from 18.91 nm to 14.00 nm, demonstrating the important role of fusion temperature in controlling nanosilica formation. The synthesized particles exhibited a quasi-spherical morphology with slight agglomeration. Overall, the results confirm that alkali fusion is an effective route for producing nanosilica from natural silica sand and that fusion temperature is a critical parameter influencing particle size and microstructural characteristics. However, further evaluation of yield, recovery, and process efficiency is necessary to support large-scale application.

Acknowledgment

This work was supported by the Institute for Research and Community Service, Universitas Tadulako.

References

[1] D. A. Rokhim, K. K. Islamiyah, and E. H. Sanjaya, "A review: analysis of metal and mineral content in the complexity of Sidoarjo hot mud as a source of renewable

[2] M. Mufti and M. Yunus, "Legal Construction of silica sand mining activities in natuna causing environmental damage impact," in Proceeding International Conference on Law, Economy, Social and Sharia (ICLESS), 2024, vol. 2, pp. 159–166.

[3] G. Kannan and E. R. Sujatha, "A review on the choice of nano-silica as soil stabilizer," Silicon, vol. 14, no. 12, pp. 6477–6492, 2022, doi: 10.1007/s12633-021-01455-z.

[4] B. A. Salami, T. A. Oyehan, Y. Gambo, S. O. Badmus, G. Tanimu, S. Adamu, S. A. Lateef, and T. A. Saleh, "Technological trends in nanosilica synthesis and utilization in advanced treatment of water and wastewater," Environ. Sci. Pollut. Res., vol. 29, no. 28, pp. 42560–42600, 2022, doi: 10.1007/s11356-022-19793-9.

[5] L. Bazzi, P. Hesemann, S. Laassiri, and S. El Hankari, "Alternative approaches for the synthesis of nano silica particles and their hybrid composites: synthesis, properties, and applications," Int. J. Environ. Sci. Technol., vol. 20, no. 10, pp. 11575–11614, 2023, doi: 10.1007/s13762-023-04845-5.

[6] P. Verma, S. Shukla, and P. Pal, "Potential application of nano-silica in concrete pavement: A bibliographic analysis and comprehensive review," Mater. Today Sustain., p. 101079, 2025, doi: 10.1016/j.mtsust.2025.101079.

[7] M. S. Hamzah, M. W. Wildan, K. Kusmono, and E. Suharyadi, "Synthesis of silica nanoparticles from silica sand via vibration assisted alkaline solution method," Int. J. Eng. Trans. A Basics, vol. 35, no. 7, pp. 1300–1306, 2022, doi: 10.5829/ije.2022.35.07a.09.

[8] P. C. Ribeiro, R. Kiminami, and A. Costa, "Nanosilica synthesized by the Pechini method for potential application as a catalytic support," Ceram. Int., vol. 40, no. 1, pp. 2035–2039, 2014, doi: 10.1016/j.ceramint.2013.07.115.

[9] A. N. Azzahra, E. S. Yusefin, G. Salima, M. Mudita, N. A. Febriani, and A. B. D. Nandyianto, "Synthesis of nanosilica materials from various sources using various methods," J. Appl. Sci. Environ. Stud., vol. 3, no. 4, p. Appl-Sci, 2020, doi: 10.48393/IMIST.PRSM/jases-v3i4.23427.

[10] S. Palagati, R. R. Kudamala, S. V Satyanarayana, J. R. Veeram, T. Garg, A. Parihar, and N. Babu, "Advanced materials synthesis by top-down and bottom-up approaches," in Advanced Materials, CRC Press, 2024, pp. 201–221.

[11] S. Palagati and J. Reddy, "Synthesis by top-down and Bottom-Up," Adv. Mater. Prod. Char. Multidiscip. App, vol. 201, 2024.

[12] S. Tripathy, J. Rodrigues, and N. G. Shimpi, "Top-down and bottom-up approaches for synthesis of nanoparticles," nanobiomaterials perspect. Med. Appl. Diagn. Treat. Dis, vol. 145, pp. 92–130, 2023, doi: 10.21741/9781644902370-4.

[13] S. Hlali, A. Kalboussi, and A. Souifi, "Nanomaterials and nanoelectronics: synthesis, properties, and applications for nanotechnology," 2025, doi: 10.5772/intechopen.1007972.

[14] Y. Zou, Z. Sun, Q. Wang, Y. Ju, N. Sun, Q. Yue, Y. Deng, S. Liu, S. Yang, and Z. Wang, "Core–shell magnetic particles: Tailored synthesis and applications," Chem. Rev., vol. 125, no. 2, pp. 972–1048, 2024, doi: 10.1021/acs.chemrev.4c00710.

[15] P. E. Imoisili, E. C. Nwanna, and T.-C. Jen, "Facile preparation and characterization of silica nanoparticles from South Africa fly ash using a sol–gel hydrothermal method," Processes, vol. 10, no. 11, p. 2440, 2022, doi: 10.3390/pr10112440.

[16] J. Maroušek, A. Marousková, R. Periakaruppan, G. M. Gokul, A. Anbukumaran, A. Bohatá, P. Kříž, J. Bárta, P. Černý, and P. Olšan, "Silica nanoparticles from coir pith synthesized by acidic sol-gel method improve germination economics," Polymers (Basel)., vol. 14, no. 2, p. 266, 2022, doi: 10.3390/polym14020266.

[17] H. Agusnar, P. Sugita, and I. Nainggolan, "Preparation sodium silicate from rice husk to synthesize silica nanoparticles by sol-gel method for adsorption water in analysis of methamphetamine," South African J. Chem. Eng., vol. 40, no. 1, pp. 80–86, 2022, doi: 10.1016/j.sajce.2022.02.001.

[18] Z. Lei, S. Pavia, and X. Wang, "Alkali-fusion as an effective method for activating low-reactivity silicate wastes: A comparative study," Constr. Build. Mater., vol. 449, p. 138504, 2024, doi: 10.1016/j.conbuildmat.2024.138504.

[19] N. S. Seroka, R. T. Taziwa, and L. Khotseng, "Extraction and synthesis of silicon nanoparticles (SiNPs) from sugarcane bagasse ash: a mini-review," Appl. Sci., vol. 12, no. 5, p. 2310, 2022, doi: 10.3390/app12052310.

[20] J. Huang, T. Liu, Y. Zhang, and P. Hu, "Comparative study of microwave-assisted and hydrothermal hydroxyapatite synthesis from neutralization slag: Optimization, energy, and adsorption," Ceram. Int., vol. 50, no. 21, pp. 42157–42168, 2024, doi: 10.1016/j.ceramint.2024.08.059.

[21] M. K. Alam, M. S. Hossain, M. Kawsar, N. M. Bahadur, and S. Ahmed, "Synthesis of nano-hydroxyapatite using emulsion, pyrolysis, combustion, and sonochemical methods and biogenic sources: a review," RSC Adv., vol. 14, no. 5, pp. 3548–3559, 2024, doi: 10.1039/D3RA07559A.

[22] M. S. Hamzah, M. W. Wildan, Kusmono, and E. Suharyadi, "Effect of sintering temperature on physical, mechanical, and electrical properties of nano silica particles synthesized from Indonesia local sand for piezoelectric application," J. Asian Ceram. Soc., vol. 11, no. 1, pp. 178–187, 2023, doi: 10.1080/21870764.2023.2173851.

[23] N. Salahudeen, "A review on zeolite: application, synthesis and effect of synthesis parameters on product properties," Chem. Africa, vol. 5, no. 6, pp. 1889–1906, 2022, doi: 10.1007/s42250-022-00471-9.

[24] N. Meftah, A. Hani, and A. Merdas, "Extraction and physicochemical characterization of highly-pure amorphous silica nanoparticles from locally available dunes sand,"

Chem. Africa, vol. 6, no. 6, pp. 3039–3048, 2023, doi: 10.1007/s42250-023-00688-2.
[25] A. Riyanto, S. Machmudah, S. Y. Purwaningsih, and S. Pratapa, “Rice husk-based silica: A structural and optical study of xerogel, amorphous, and crystalline phases,” Opt. Mater. (Amst)., p. 117115, 2025, doi: 10.1016/j.optmat.2025.117115.
[26] A. R. Aidid, M. K. H. Shishir, M. A. Rahaman, M. T. Islam, M. Mukta, and M. A. Alam, “Powder X-ray line diffraction pattern profiling of anatase-quartz binary oxide: A crystallographic investigation,” Next Mater., vol. 8, p. 100571, 2025, doi: 10.1016/j.nxmate.2025.100571.
[27] F. D. M. Daud, M. H. Johari, A. H. A. Jamal, N. A. Z. Kahlib, and A. L. Hairin, “Preparation of nano-silica powder from silica sand via sol-precipitation method,” in AIP Conference Proceedings, 2019, vol. 2068, no. 1, p. 20002, doi: 10.1063/1.5089301
[28] H. N. Kim and K. S. Suslick, “The effects of ultrasound on crystals: Sonocrystallization and sonofragmentation,” Crystals, vol. 8, no. 7, p. 280, 2018, doi: 10.3390/cryst8070280.